


Article

Recovery of Rare Earth Elements Minerals in Complex Low-Grade Saprolite Ore by Froth Flotation

George Blankson Abaka-Wood ^{1,2,*} , Bob Johnson ³, Jonas Addai-Mensah ^{1,4} and William Skinner ^{1,2}

¹ Future Industries Institute, University of South Australia, Mawson Lakes Campus, Adelaide, SA 5095, Australia

² ARC Centre of Excellence for Enabling Eco-Efficient Beneficiation of Minerals, University of South Australia Node, Adelaide, SA 5095, Australia

³ Maptek Pty. Limited, Adelaide, SA 5065, Australia

⁴ Department of Mining and Process Engineering, Namibia University of Science and Technology, Jackson Kaujeua Street, Windhoek 13388, Namibia

* Correspondence: george.abaka-wood@unisa.edu.au

Abstract: This study presented the first in a series of investigations currently underway to develop efficacious, cost-effective, and benign processing opportunities to produce rare earth elements (REE)-rich concentrate from an Australian complex low-grade saprolite ore [1.14% total rare earth oxides (TREO) grade], which is primarily exploited for its gold and copper values. This work specifically presented a preliminary flotation investigation carried out on the ore using sodium oleate as a collector. The relative effects of pulp pH, desliming, and depressants were investigated to ascertain any chance of recovering and upgrading REE minerals in saprolite ore using three different processing configurations. Based on the experimental results, flotation processes carried out on raw feed allowed the recovery of the majority of REE minerals (>50%), but the process was unselective, where clay and silicate gangue minerals reported into the flotation concentrate along with the REE minerals. However, desliming before flotation in the presence of depressants (starch and sodium silicate) improved REE minerals flotation selectivity, which produced concentrates assaying 5.87% and 4.22% TREO grades, with corresponding recoveries of 45% and 50% at pulp pH 9 and 10.5, respectively. Mineralogical analysis conducted on selected flotation concentrate indicated that silicate and clay gauge minerals were recovered via the synergistic act of surface activation and entrainment due to their fine to ultrafine nature. A comparison of all the test results revealed a haphazard grade-recovery relationship suggesting that there is an opportunity to further maximize both REE recovery and grade through further flotation studies where other process parameters may be investigated and optimized. The prospect of using magnetic separation has also been suggested.

Keywords: bastnäsite; desliming; froth flotation; quartz; saprolite ore



Citation: Abaka-Wood, G.B.; Johnson, B.; Addai-Mensah, J.; Skinner, W. Recovery of Rare Earth Elements Minerals in Complex Low-Grade Saprolite Ore by Froth Flotation. *Minerals* **2022**, *12*, 1138. <https://doi.org/10.3390/min12091138>

Academic Editor: Hyunjung Kim

Received: 30 July 2022

Accepted: 29 August 2022

Published: 8 September 2022

Publisher's Note: MDPI stays neutral with regard to jurisdictional claims in published maps and institutional affiliations.



Copyright: © 2022 by the authors. Licensee MDPI, Basel, Switzerland. This article is an open access article distributed under the terms and conditions of the Creative Commons Attribution (CC BY) license (<https://creativecommons.org/licenses/by/4.0/>).

1. Introduction

Rare earth elements (REE) are abundant in the Earth's crust, usually mineralized with bastnäsite, monazite, florencite, xenotime, and ion adsorption clays; however, economic grades are comparatively less common than most valuable minerals and metals [1–3]. Most of the global rare earth oxides (REO) production presently comes from four countries: China accounting for about 60% of global production, the U.S.A. with nearly 16%, followed by Burma and Australia with about 9% and 8%, respectively [4]. It is worth noting that the production rates may be adequate to meet the current global demand; however, potential REE supply risk is real due to the geographic concentration of REO production and the growing demand for green energy and high-tech appliances [4–8]. Consequently, although substitute elements may be available for many applications, they have been reported to be less effective with significant limitations [3,4,9].

The demand for REEs in the global market has been increasing for the past three decades due to their technological and industrial applications. The crucial drivers for the increasing REE demand include permanent magnet applications, rechargeable batteries, and phosphors due to the role they play in green energy and high-level technology applications [2,10–12]. Currently, bastnäsite $[(\text{Ce}, \text{Nd}, \text{Y}, \text{REE})(\text{CO}_3)\text{F}]$ and monazite $[(\text{Ce}, \text{La}, \text{Nd})\text{PO}_4]$ are the most important commercially exploitable REE minerals, which are usually found in association with different gangue minerals including hematite (Fe_2O_3), quartz (SiO_2), muscovite $[(\text{KF})_2(\text{Al}_2\text{O}_3)_3(\text{SiO}_2)_6]$, goethite $[\text{FeO}(\text{OH})]$, and carbonate gangue minerals based on the geographical location and activities [5,13–17].

Beneficiation (e.g., froth flotation, magnetic separation, gravity separation) of REE minerals have become increasingly complicated, especially where ore grade is significantly low [$<1\%$ total REO (TREO)]. Typically, low-grade ores are dominated by fine- to ultrafine gangue minerals, including silicates, carbonates, and phosphates. To this end, one of the major drawbacks is developing robust, efficient methods for reducing the proportion of gangue minerals that are reported into concentrates generated from the various beneficiation methods [1,2,5,7]. The presence of high gangue minerals limits the use of direct hydrometallurgical and pyrometallurgical processes to extract REE.

Most REE minerals prospected in Australia are enriched within the fine- to ultrafine ore fractions ($<38\ \mu\text{m}$). This challenge is exacerbated by the fact that most gangue minerals tend to form complex composite particles with REE minerals even at such fine sizes. This challenge has deleterious impacts on the efficiency of most preconcentration and beneficiation processes, as demonstrated in previous studies [18–21].

Although current research and development studies are focused on resolving these challenges in the recovery of REE minerals from very complex resources, these drawbacks remain unresolved, as they are usually ore specific. Thus, some proposed solutions may not be generalized for all REE-bearing ores, as they differ physically, chemically, and mineralogically. For example, the processing response of REE minerals hosted in an iron oxide copper gold (IOCG) deposit will differ significantly from those deported into saprolite ores, coal ash, red mud, or phosphogypsum materials. In effect, addressing these challenges associated with REE mineral recovery requires an ore-specific approach where the material is chemically and mineralogically characterized, which will then be followed by designing beneficiation and extraction processes to recover REE values.

The present study was carried out on selected Australia saprolite ore, which is currently being developed for gold and copper extraction. Preliminary characterization studies have highlighted the potential of recovering REE as a by-product of the primary commodities. As part of ongoing Research and Development studies, the prospect of recovering REE minerals from the ore was investigated.

Specifically, the aim of this study was to identify the processing opportunities for recovering REE minerals by froth flotation while examining the mineralogical characteristics of the feed and selected separation products. Process combinations to improve REE minerals recovery and upgrade were studied using three simple flowsheets, which sought to unravel the relative impacts of pulp pH, depressants addition, and desliming on REE recovery and upgrade. Also, this work set in motion possible avenues which can be explored in the future to enhance REE minerals recovery and upgrade from the ore.

2. Materials and Methods

2.1. Materials

An Australian saprolite ore was used in this study. All reagents were prepared in Milli Q water. In the flotation tests, sodium oleate (Sun Ace, Dandenong South VIC, Australia) and Methyl Isobutyl Carbinol (MIBC) were used as a collector and frother, respectively, while sodium silicate (Coogee Chemicals, Kwinana Beach, WA, Australia) and starch (Grain Processing Corporation, Muscatine, IA, USA) were used as depressants. Sodium oleate and starch were solubilized with 10 wt.% sodium hydroxide (NaOH) solution under magnetic stirring for about 20 min, followed by the addition of distilled water. Flotation pulp feed

was prepared by mixing the ore with Adelaide tap water, where the pulp pH was adjusted to the desired level using dilute solutions of hydrochloric acid and sodium hydroxide. To obtain suitable feed for the investigation, a known mass of the feed was mixed with water and screened into two size fractions; +150 μm and –150 μm , where the barren (i.e., +150 μm) fraction was not considered for subsequent beneficiation studies. The –150 μm fraction served as feed for all the tests carried out in this study. When required, a Mozley hydrocyclone was used for desliming the feed.

2.2. Ore Characterization

To de-agglomerate the feed, a representative subsample (1 kg) of the ore was mixed with Adelaide tap water to generate 30 wt.% pulp for about 30 min. About 500 mL pulp sample was obtained, filtered, dried, and analyzed. Chemical analysis was carried out using an inductively coupled plasma mass spectrometry (ICP-MS), whereas the mineralogical composition of the samples was analyzed via X-ray powder diffraction (XRD) and Quantitative Evaluation of Materials by Scanning Electron Microscopy (QEMSCAN) analyses. The slime fraction of the feed (–10 μm) was removed prior to QEMSCAN analysis. Approximately 2 g sample was subsequently presented for particle size distribution analysis using a laser diffraction method with Malvern Mastersizer 2000 (Malvern Panalytical, Malvern, UK). Furthermore, a representative subsample was obtained from the bulk of the pulp, and wet screened, where the respective particles retained on the screens were dried and analyzed for their chemical composition.

2.3. Bulk Froth Flotation

Flotation tests were carried out using a 500 mL Denver cell (Denver Equipment Company, Colorado Springs, CO, USA), where the impeller speed (1000 rpm) and air flow rate (1.5 dm^3/min) were maintained during the conditioning and flotation stages. During the flotation tests, the desired dosage of sodium oleate was added with 5 min conditioning time, followed by 2 drops of 1% MIBC with 1 min conditioning time. Throughout the flotation tests, the froths were collected every other 0.25 min over 10 min. Where depressants were required, the desired concentration was added with 5 min conditioning time prior to the addition of the collector and frother. The flotation products were then filtered, dried overnight at 50 °C in an electric oven, weighed, and assayed using ICP-MS analysis. The recovery and grade of TREO and gangue species recovery were calculated as outlined in previous studies [18]. Details of the flotation processes tested are outlined below and presented in Figure 1.

- Flowsheet I: Direct flotation tests were conducted at pulp pH 9 and 10.5 in a single-stage rougher flotation test using 3000 g/t sodium oleate. This was to assess the flotation response of REE and gangue species at pH 9, which has been widely reported in the literature to be suitable for REE recovery using fatty acids as collectors [22–24]. Pulp pH 10.5 was selected to assess the feasibility of recovering REE minerals as a by-product of gold leaching, which is typically carried out at pH range of 10–11 [25–27].
- Flowsheet II: In this process, the feed was deslimed and subsequently floated at pH 9 and 10.5 in the absence of sodium silicate and starch as depressants, respectively. This was performed with the view of selectively rejecting a significant proportion of the gangue minerals, which were reported into the flotation concentrates generated when Flowsheet I was tested. The aim of this process was to assess the relevance of desliming stage in the recovery of REE minerals in the ore.
- Flowsheet III: A rougher-scavenger-cleaner method was tested on deslimed feed at pulp pH 9 and 10.5 in the presence of depressants to assess any chance of improving REE mineral selectivity. The process commenced with a rougher flotation stage, where 5000 g/t sodium oleate was used in the presence of 1500 g/t sodium silicate and 1500 g/t starch, followed by the scavenging of the rougher tailings. In the final step, the rougher and scavenger concentrates were combined and cleaned with 1500 g/t sodium silicate and 1500 g/t starch.

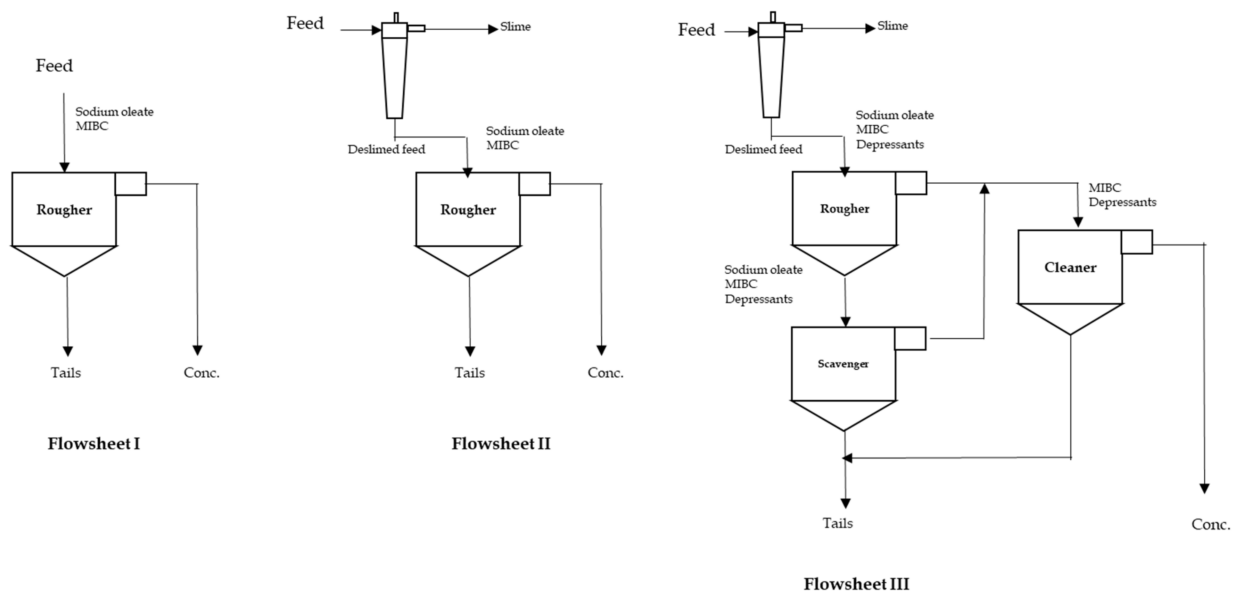


Figure 1. Schematic representation of the flotation flowsheets used in this study.

3. Results

3.1. Physicochemical Characteristics of the Ore

3.1.1. Particle Size Distribution

Particle size distribution of the ore presented in Figure 2 showed that typical for a highly weathered ore, the material was dominated by fine and ultrafine particles, with P_{50} approximately 7 μm and 80% of the feed finer than 20 μm .

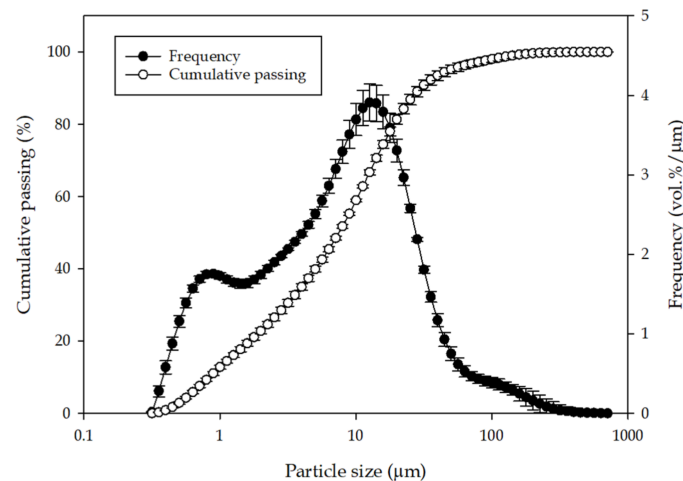


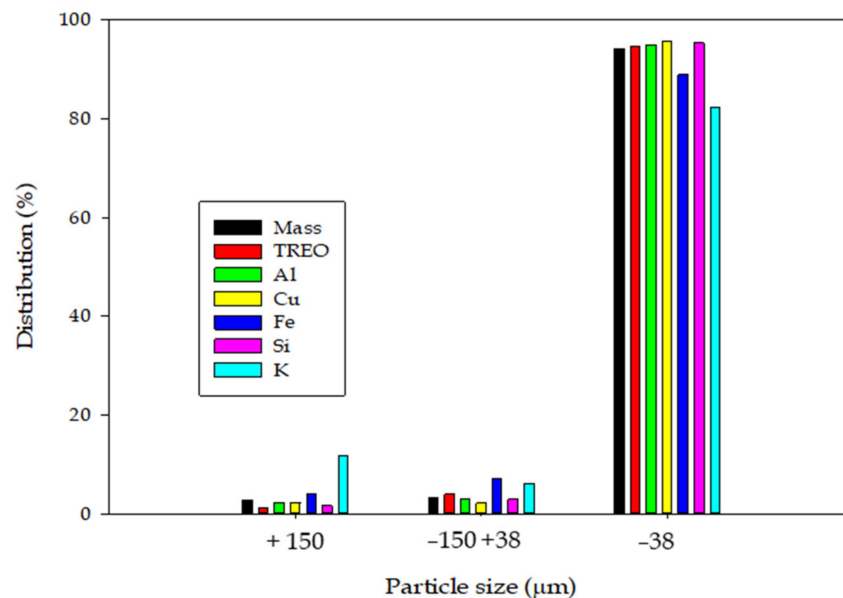
Figure 2. Particle size distribution of representative feed sample obtained via laser diffraction method.

3.1.2. Chemical Composition

Results obtained from ICP-MS analysis conducted on the feed sample are shown in Table 1. Chemical analysis of the head sample indicated that the ore contained 22.25% Si, 13.8% Al, and 2.83% Fe as key gangue species. Of key interest to this study, the TREO content assayed 1.142%, with the light rare earth oxides (LREO) composing about 82% of the TREO. To ascertain the distribution of REE in the ore, representative subsamples were wet screened, and each size fraction was analyzed for its REE content along with key gangue elements, as shown in Figure 3.

Table 1. Summary of results obtained from ICP-MS analysis.

Rare Earth Oxides	Content (%)	Gangue Species	Content (%)
La ₂ O ₃	0.366	Al	13.8
Sc ₂ O ₃	0.002	Ca	0.14
CeO ₂	0.092	Cu	0.70
Dy ₂ O ₃	0.020	Fe	2.83
Er ₂ O ₃	0.008	K	1.48
Eu ₂ O ₃	0.012	Mg	0.63
Gd ₂ O ₃	0.044	Na	1.16
Ho ₂ O ₃	0.003	P	0.04
Lu ₂ O ₃	0.001	Si	22.25
Nd ₂ O ₃	0.328		
Pr ₆ O ₁₁	0.086		
Sm ₂ O ₃	0.057		
Y ₂ O ₃	0.113		
Yb ₂ O ₃	0.005		
Tb ₄ O ₇	0.005		
TREO	1.142		

**Figure 3.** Mass, TREO, and selected major gangue elements distribution in the ore.

It could be deduced that the REE content in each size fraction followed the mass yield, which suggested that REE is evenly disseminated in the various size fractions. A similar trend was noticed for all the gangue elements. In effect, the bulk of REE in the ore was concentrated within the fine fraction (<38 μm), which accounted for 94.7% and 94.1% of the TREO and mass, respectively. To this end, no upgrade was achieved within the respective size fractions. The coarse fraction (>38 μm) was subsequently screened out, and all flotation tests were conducted on the fine fraction (<38 μm).

3.1.3. Mineralogical Composition

Bulk mineralogical analysis was carried out on a representative feed subsample using XRD, and the results are summarized in Table 2. The ore contained a high proportion of silicate and clay gangue minerals, with the analysis unable to detect REE-bearing minerals. This may be because of the complex nature of the ore, coupled with the significantly low REE content, which made them undetectable.

Table 2. Modal mineralogy of the feed determined via XRD analysis.

Mineral	Abundance (wt.%)
Quartz	6
Hematite group	<1
Kaolinite-serpentine group	10
Anatase	<1
Rutile group	2
Plagioclase	5
K feldspar	32
Smectite Group	6
Barite Group	1
Mica group	4
Amorphous	32
Total	100

3.2. Froth Flotation

Results obtained from the various flowsheets (I–III) are summarized in this section, where mass yield, TREO recovery, and grade and key gangue species (Al, Fe, and Si) recovery are compared.

3.2.1. Baseline Flotation (Flowsheet I)

Previous flotation studies conducted by Filippov et al. [20], Satur et al. [21], and Abaka-Wood et al. [28] have suggested that high REE recovery could be achieved using fatty acids as a collector at pulp pH > 8. To assess the flotation response of the ore, Flowsheet I was tested where sodium oleate dosage was maintained at 3000 g/t at pH 9 and 10.5, respectively. The flotation performances have been summarized in Figures 4 and 5, where the TREO, Si, Fe, and Al recoveries are compared. TREO recoveries obtained follow the mass yield and gangue species recoveries. It can also be deduced from the data that higher recoveries were achieved in tests conducted at pH 10.5, which is consistent with that observed by Satur et al. [21].

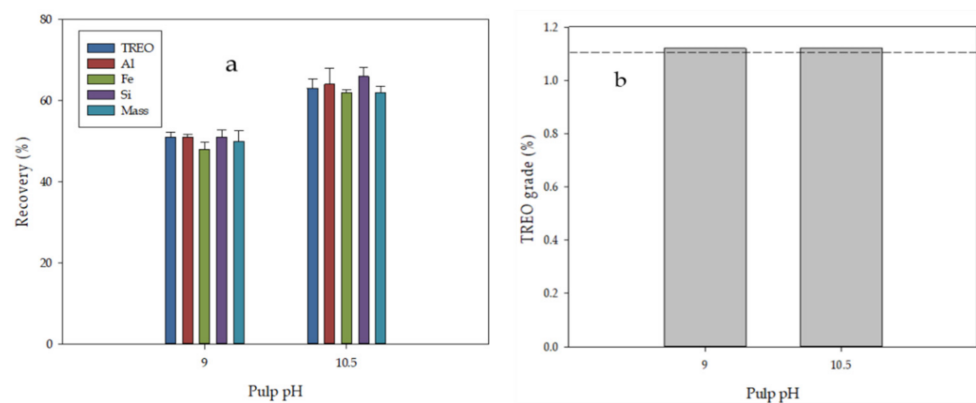


Figure 4. (a) TREO, mass, and gangue species recoveries and (b) TREO grade as a function of pulp pH 9 and 10.5 (dash line represents feed grade = 1.14% TREO).

As demonstrated in the literature, sodium oleate is selective against silicate minerals [28,29]; hence the silicate minerals may have been recovered via mechanical entrainment. Consequently, the poor TREO concentrate grade obtained is a testament to the high gangue recoveries via entrainment. Overall, the performance of the flotation tests conducted on the “as received” feed was poor due to the high gangue species recovery via entrainment, which contrasted with previous tests that showed remarkable REE recoveries and upgrades at mild to strong alkaline pulp pH conditions [16,23]. These results demonstrated the need for surfactants capable of selectively coating the surface of gangue silicate minerals to

inhibit their recovery. Prior to that, the avenue to explore the removal of barren ultrafine silicate and clay minerals was considered in subsequent tests.

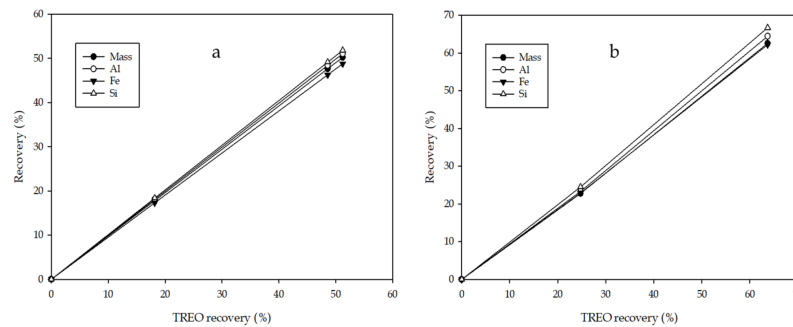


Figure 5. TREO–mass and selected gangue species recoveries relationship in concentrates obtained at (a) pH 9 and (b) pH 10.5.

3.2.2. Desliming followed by Flotation (Flowsheet II)

In an attempt to address the issue of entrainment, the impact of particle size distribution became crucial. As it has been suggested and confirmed, ultrafine (<50 μm) gangue minerals largely misreport into flotation concentrates by entrainment [5,30–32]. Hence, an alternative method that includes desliming needs to be considered. A representative feed sample (1 kg) was processed via a hydrocyclone in an attempt to remove the slimes in the material. Figure 6 shows the particle size distribution of the cyclone products, and Table 3 provides their chemical composition. The results demonstrated that more than half of the flotation feed was finer than 10 μm, which was reported with the overflow as slimes. Most importantly, the majority of the REE minerals reported with the cyclone underflow, which was desirable, resulting in a significant TREO upgrade. Also, most of the silicate minerals are reported into the slime fraction. Thus, the desliming process removed up to 51% silicate gangue minerals while recovering about 89% TREO into the cyclone underflow, with a significant increase in grade from 1.34% to 2.71%.

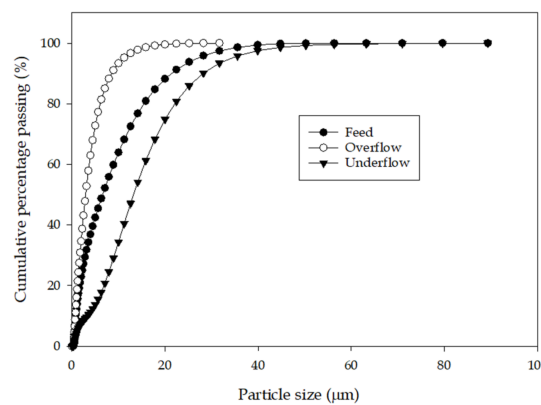


Figure 6. Particle size distribution of hydrocyclone feed and products obtained via laser diffraction method.

Table 3. Results of desliming tests conducted on flotation feed.

Product	d ₅₀ (μm)	d ₈₀ (μm)	Mass (%)	TREO		Si		Fe		Al	
				Dist. (%)	Grade (%)	Dist. (%)	Grade (%)	Dist. (%)	Grade (%)	Dist. (%)	Grade (%)
Underflow	13.2	28.4	44	89	2.71	49	24.72	82	5.04	40	9.92
Overflow	3.0	8.4	56	11	0.26	51	20.31	18	2.17	60	12.75
Feed (calc.)	7.3	33.3	100	100	1.34	100	22.25	100	2.70	100	10.89

Flotation tests were subsequently conducted on the deslimed feed (cyclone underflow) in the absence of depressants, and the results are summarized in Table 4. There was a clear, significant improvement in the TREO upgrade, although recoveries decreased slightly. Similar to what was observed in Flowsheet I, a comparatively higher TREO recovery was achieved at pH 10.5, where 51% TREO recovery was achieved at a concentrate grade of 4.22%. On the other hand, a higher TREO concentrate grade of 5.87% at 45% recovery was achieved at pH 9. The higher concentrate grade achieved at pulp pH 9 may be attributed to the lower proportion of gangue minerals that were misreported into the flotation concentrate.

Table 4. Summary of results obtained for Flowsheet II at pH 9 and 10.5.

Product	Yield (%)	Grade (%)				Recovery (%)			
		TREO	Fe	Al	Si	TREO	Fe	Al	Si
<i>pH 9</i>									
Feed	100	2.71	5.04	9.92	24.72	100	100	100	100
Conc.	21	5.87	3.16	11.28	22.11	45	13	24	19
Tails	79	1.87	5.54	9.56	25.43	55	87	76	81
<i>pH 10.5</i>									
Feed	100	2.71	5.04	9.92	24.72	100	100	100	100
Conc.	33	4.22	2.66	10.88	23.59	51	17	36	31
Tails	67	1.97	6.21	9.45	25.29	49	83	64	69

3.2.3. Desliming–Flotation in the Presence of Depressants (Flowsheets III)

As a follow-up on the impressive results obtained from Flowsheet II, Flowsheet III was developed. In this beneficiation route, a blend of conventional depressants (sodium silicate and starch) was tested in the presence of sodium oleate at pulp pH 9 and 10.5, respectively. Both depressants were effective in reducing the recovery of gangue minerals in flotation systems where selective REE minerals recovery was desired [21,23,24,33,34].

Flowsheet III at pH 9

The multistage flotation process at pH 9 produced a reasonably satisfactory performance (Table 5). Overall, the final concentrate recovered 59% TREO, which was comparatively higher than that obtained in Flowsheet II at pH 9. However, in terms of upgrade, the concentrate grade obtained in Flowsheet III (5.14% TREO) was slightly lower than that obtained in Flowsheet II (5.87% TREO). In terms of gangue rejection, the results were less favorable compared with the direct rougher flotation tests (Flowsheet II) because higher proportions of Al, Fe, and Si were reported into the final concentrates, which could be responsible for the comparatively lower TREO upgrade although a higher recovery was obtained.

Table 5. Summary of results obtained for Flowsheet III at pH 9.

Product	Yield (%)	Grade (%)				Recovery (%)			
		TREO	Fe	Al	Si	TREO	Fe	Al	Si
<i>Rougher</i>									
Feed	100	2.71	5.04	9.92	24.72	100	100	100	100
Conc.	23	3.93	2.71	10.63	22.90	33	12	25	21
Tails	77	2.35	5.74	9.71	25.28	67	88	75	79
<i>Scavenger</i>									
Conc.	51	2.79	2.78	10.61	22.90	53	28	55	47
Tails	26	1.48	11.53	7.94	29.94	14	60	20	32

Table 5. Cont.

Product	Yield (%)	Grade (%)				Recovery (%)			
		TREO	Fe	Al	Si	TREO	Fe	Al	Si
<i>Rougher</i>									
<i>Cleaner (Feed comprise rougher and scavenger concentrates)</i>									
Feed	74	3.23	2.76	10.62	22.90	86	40	79	69
Conc.	30	5.14	2.43	9.57	21.03	55	14	29	26
Tails	44	1.93	2.98	11.33	24.18	30	26	50	42

Flowsheet III at pH 10.5

The process followed the exact same route as Flowsheet III at pulp 9, and the results obtained are summarized in Table 6. Lower TREO recoveries and upgrades were obtained at pulp pH 10.5. For instance, the multistage flotation process produced a final cleaner concentrate with 2.95% TREO at 32% recovery compared with the cleaner concentrate produced at pH 9, which contained 5.14% TREO at 55% recovery.

Table 6. Summary of results obtained for Flowsheet III at pH 10.5.

Product	Yield (%)	Grade (%)				Recovery (%)			
		TREO	Fe	Al	Si	TREO	Fe	Al	Si
<i>Rougher</i>									
Feed	100	2.71	5.04	9.92	24.72	100	100	100	100
Conc.	71	2.48	2.71	9.52	23.51	65	38	68	67
Tails	29	3.28	10.74	10.90	27.72	35	62	32	33
<i>Scavenger</i>									
Conc.	6	3.39	3.18	9.29	19.44	7	4	6	5
Tails	23	3.25	12.72	11.32	29.88	28	58	26	28
<i>Cleaner (Feed comprise rougher and scavenger concentrates)</i>									
Feed	77	2.57	2.75	9.50	23.24	72	42	74	72
Conc.	30	2.95	2.50	9.57	23.0	32	15	29	28
Tails	47	2.33	2.91	9.46	23.4	40	27	45	44

Comparing the data in Tables 4–6, a general decrease in gangue species recovery was observed when the multistage flotation tests were conducted in the presence of depressants. Interestingly, identical gangue species recoveries were observed at both pH 9 and 10.5 when Flowsheet III was tested.

Figure 7 summarizes the flotation efficiency index (E) of the respective flowsheets, calculated using the expression

$$E = [((R - \gamma)/(100 - \alpha))] \times 100\% \quad (1)$$

where R is TREO recovery and γ is the yield of concentrate, and α is the TREO content in the raw feed. Generally, better flotation efficiencies were obtained at pulp pH 9 when compared to pH 10.5. The data suggested that the highest flotation performance was achieved when Flowsheet III was tested at pH 9, followed by Flowsheet II at pH 9. Hence, the final concentrate obtained from Flowsheet III and tested at pH 9 was selected for subsequent mineralogical analysis.

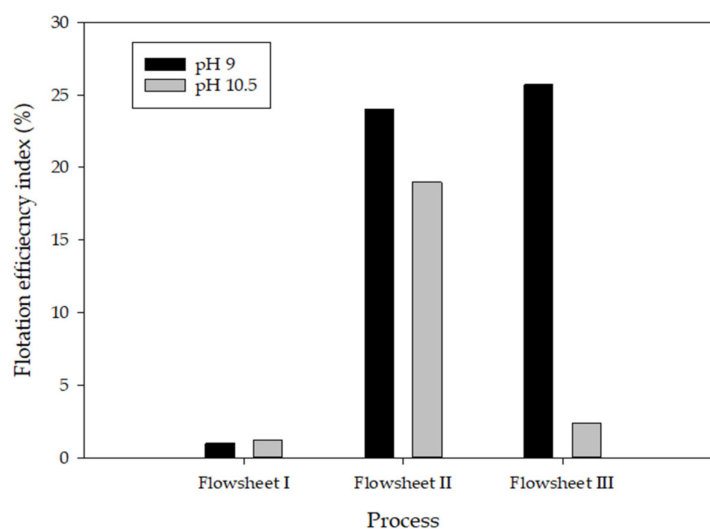


Figure 7. Flotation efficiency index of Flowsheets I–III.

3.3. Mineralogical Composition of Flotation Feed and Concentrate

The deslimed feed and final concentrate obtained from Flowsheet III at pH 9 were analyzed for their mineralogical composition to provide detailed knowledge on the REE and gangue minerals recovered, their association, size distribution, and liberation characteristics.

3.3.1. Modal Mineralogy

The mineral abundance data of the selected samples obtained via QEMSCAN analysis are listed in Table 7. The data demonstrated an appreciable level of REE minerals recovery and upgrade, with a total REE minerals content increase from 8.5% in the deslimed feed to 14.3% in the flotation concentrate. The main REE mineral present was bastnäsite, with different REE intergrowths and a trace amount of monazite. The REE intergrowths (including La-Nd-Si, La-Fe, and REE intergrowths) have similar characteristics to REE associated with ion adsorption clays [35–37]. The data generally suggested that the REE phases were enriched in the concentrates, except for monazite. For instance, the analysis reported an increase in bastnäsite abundance from 3% to 5.6% in the concentrate. A similar increase in abundance was observed for La-Nd-Si intergrowths, where an upgrade from 3.7% to 6.3% was observed. In addition, the bulk of the flotation concentrate was occupied by silicate and clay minerals which explains the low REE value upgrade, although recovery was high. Despite occupying the bulk fraction of the concentrate, the data suggested a decrease in the concentration of clay and silicate minerals in the concentrate compared with their respective concentrations in the feed.

Table 7. Mineralogical composition of deslimed flotation feeds and concentrates.

Mineral	Mineral Mass (%)	
	Deslimed Flotation Feed	Flotation Concentrate
Monazite and intergrowths	0.1	0.1
Bastnäsite	3.0	5.6
La-Nd-Si intergrowths	3.7	6.3
La-Fe intergrowths	0.9	1.0
REE intergrowths	0.8	1.3
* Total REE minerals	8.5	14.3
Iron oxide/hydroxide (FeO _x /OH)	0.4	0.9
Sulphates	0.5	1.8
Ti minerals	1.3	2.2

Table 7. Cont.

Mineral	Mineral Mass (%)	
	Deslimed Flotation Feed	Flotation Concentrate
Quartz	7.9	7.9
Clays	22.3	21.9
Micas	19.0	18.0
K silicates	10.0	7.2
Fe silicates	1.9	1.8
Na silicates	24.7	20.7
Other silicates	3.3	3.1
Others	0.2	0.3
Total	100	100

* Sum of REE minerals/phases.

3.3.2. Mineral Liberation

The extent of REE minerals liberation was important as it provided key information which may be useful in understanding the efficiency of beneficiation processes. With REE mineral recovery the focus of this investigation, the liberation and locking data of combined REE and silicate phases, respectively, are presented in Figure 8. The data suggested varying liberation characteristics of the two groups of minerals. More than 90% of silicate particles were completely liberated in both the feed and concentrate. In the case of REE minerals, the data suggested that REE particles reported into the concentrates were slightly more liberated than those in the feed. Overall, a little under half of the REE minerals (40–45%) were completely liberated within the feed and concentrate, with the remaining particles forming middling and locked composite particles with the gangue minerals.

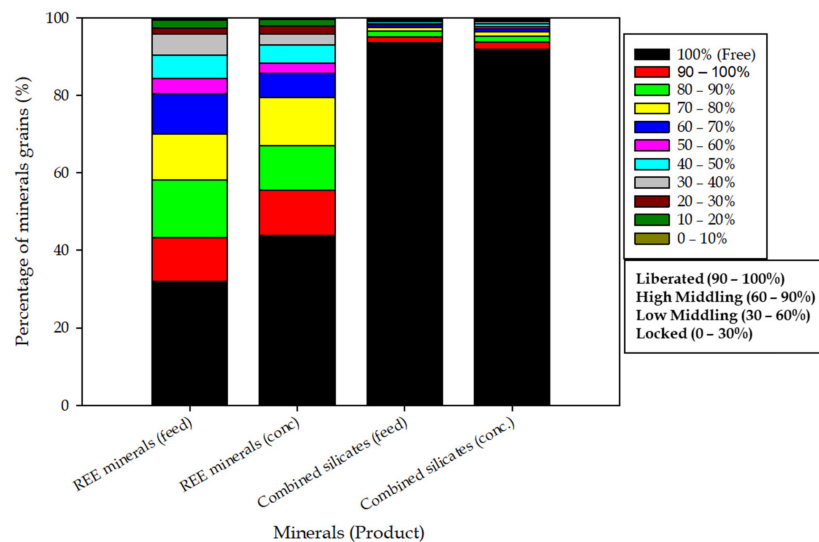


Figure 8. Liberation of the combined REE-bearing minerals and combined silicates in the flotation feed and concentrate.

3.3.3. Minerals Grain Size

Particles are typically made of mineral grains; hence the average grain sizes determined via QEMSCAN is an estimate of the diameter of the mineral grains. In this investigation, the estimated value was the diameter of a sphere of equivalent volume to the average particles in the measured population. Characteristically, mineral grains are hardly spherical; hence the actual grains could be either coarser or finer than the estimated sizes in different axes or orientations.

The QEMSCAN grain size distribution and average P₈₀ of REE and silicate minerals are shown in Figure 9. The data suggested that both phases were fine, with almost identical

grain sizes. For instance, REE minerals grains had an estimated P_{80} of 24 μm , whereas the silicate had an estimated P_{80} of 20 μm . The fine nature of silicate minerals has been reported to have detrimental effects on flotation processes including selectivity, high reagents consumption, and poor concentrate grade [21,31,38,39]. The data presented in Figure 9 was confirmed by the particle view of the flotation concentrate obtained via QEMSCAN shown in Figure 10, which generally presented fine silicates (quartz, K silicate, Na silicates, other silicates, and mica), clay, and REE phases.

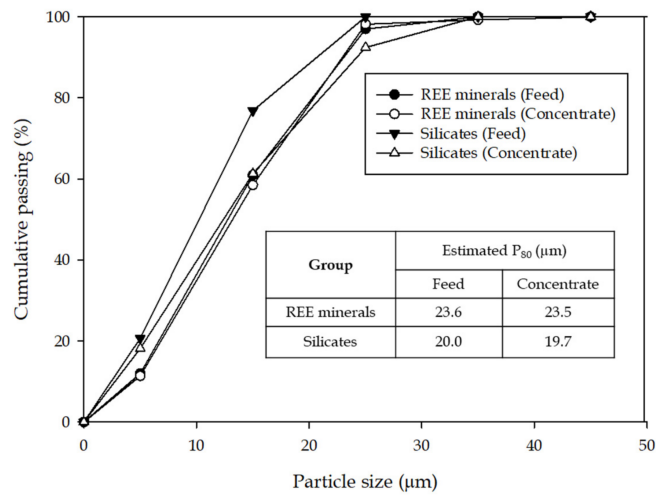


Figure 9. Grain size distribution of REE and silicate minerals in flotation feed and concentrate.

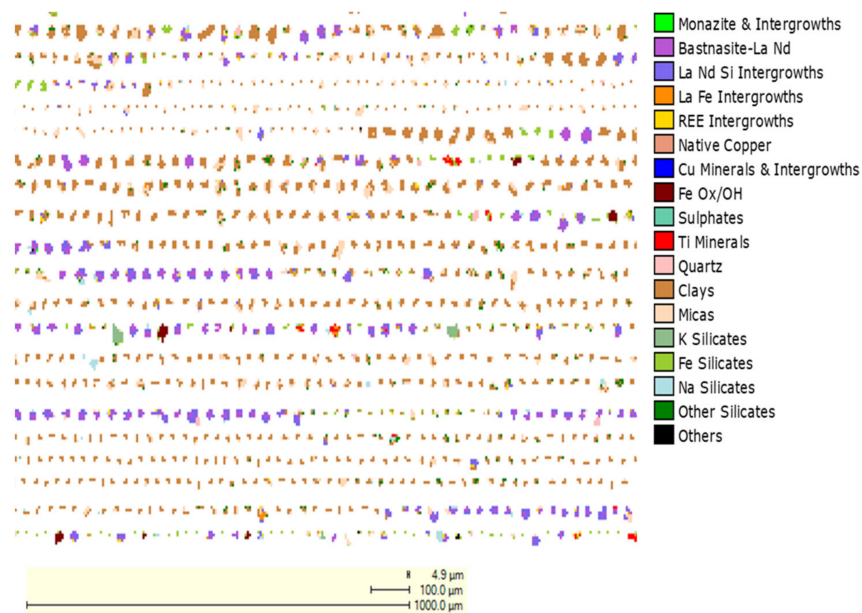


Figure 10. Particle view of the flotation concentrate.

4. Discussion

4.1. The Role of Pulp pH

Pulp chemistry, governed by pH, plays a crucial role in the flotation of minerals. pH typically controls the surface charge of minerals; interfacial reactions between mineral particles and reagents; and particle–particle interactions. These interfacial reactions may result in the selective flotation of minerals and in some cases may lead to poor flotation performance. In principle, the right balance between reagent concentrations and pulp pH is key in achieving the flotation selectivity of valuable minerals in complex ores [29,40].

This was evident in the tests conducted on both raw and deslimed feed samples. For instance, the obtained results have shown higher REE recoveries at pH 10.5 in the rougher flotation tests, which corroborated with tests conducted by Satur et al. [21]. The flotation study conducted by Satur et al. [21] on silicate-hematite ore using a tall oil fatty acid collector, showed better REO recoveries at pH 10.5 compared with pH 9. Elsewhere, works by Pavez et al. [32], Cheng et al. [41], and Zhang et al. [42] showed conflicting results where REE recoveries declined in strong alkaline pulp conditions. For example, tests on coal by Zhang et al. [42] showed that REE recovery and upgrade were achieved at pH 9, where a further increase in pulp pH saw a decline in flotation performance. The conflicting results from the various studies confirm the need to design ore-specific methods to recover their valuable REE content.

4.2. Surface Activation of Silicate and Clay Minerals

Flotation tests conducted on the raw feed showed higher REE and gangue species recoveries, with associated poor TREO upgrade. The strong alkaline pulp condition and the presence of polyvalent cations created suitable conditions for the flotation of silicate and clay minerals. It is well documented in the literature that the solubility of oleate ions increases with a corresponding increase in pH, where oleate species mainly exist in the form of oleate ion (RCOO^-) and oleate dimer ($(\text{RCOO})_2^{2-}$) typically at $\text{pH} > 10$ [43–45]. Oleate ions can interact with the silicate minerals surfaces activated by polyvalent metal cations to promote flotation recovery. The liberation data (Figure 8) indicated that the silicates have high (>90%) surface exposure which could promote surface activation by different cations, coupled with REE cations adsorbed onto clay minerals, mainly due to the large surface area to volume ratio and negatively charged surfaces [36,46]. These are partly responsible for the high silicate and clay minerals recoveries observed in the present study, although oleate ions cannot directly adsorb onto the clay and silicate minerals surface [24,29,47].

4.3. Effect of Mineral Grain Size

The recovery of silicates and clay minerals was exacerbated by their free (Figure 8), fine-, or ultrafine nature (Figures 9 and 10). Grain size distribution data obtained via QEMSCAN analysis revealed that the silicate gangue minerals have a combined $P_{80} < 25 \mu\text{m}$, making them susceptible to mechanical recovery, which was undesirable. It has been demonstrated in the literature that gangue mineral particles finer than $50 \mu\text{m}$ were easily recovered into flotation concentrates via entrainment [48,49]. Elsewhere, studies by Wang et al. [50] have demonstrated the recovery of typical gangue minerals due to their fine- or ultrafine nature. Consequently, the increased entrainment recovery of fine- or ultrafine gangue minerals is known to reduce the quality of flotation concentrates even when depressants are used [51]. With >90% silicate minerals completely liberated from REE and Fe bearing minerals, the silicate particles may be regarded as “barren”, which suggests that their high content in the flotation concentrate cannot be mainly attributed to composite association with value minerals as observed in previous studies by Filippov et al. [20] and Abaka-Wood et al. [51]. To this effect, the fine- or ultrafine nature and surface activation of silicate and clay minerals promoted the recovery of gangue minerals. To date, there have been increased efforts to minimize entrainment recovery of fine gangue minerals with Jameson cell and Reflux flotation cell [52–54], which may be considered in the near future to process the ore used in this study.

4.4. Relevance of Desliming

Desliming in mineral processing has wide range of applications with different impacts on various beneficiation flowsheets. It has significantly contributed to the upgrade of mineral values thus confirming its attractiveness in flowsheet development where slimes impede value upgrades [55]. Elsewhere desliming has been reported to contribute to some value losses [56,57]. In the present study, significant gains in desliming prior to the flotation process were observed as shown in Figure 11. For instance, there was an improvement

in REE selectivity, which resulted in a comparatively better upgrade than when the raw feed was processed. The selectivity curves skewed towards the TREO recovery axis for all the deslimed feed curves, whereas the data points remained in the center (gradient and selectivity ~1) for tests conducted on the raw feed. Table 8 presents a summary of the selectivity indices obtained for tests conducted on both raw and deslimed feeds, calculated as the gradient of the various curves in Figure 11.

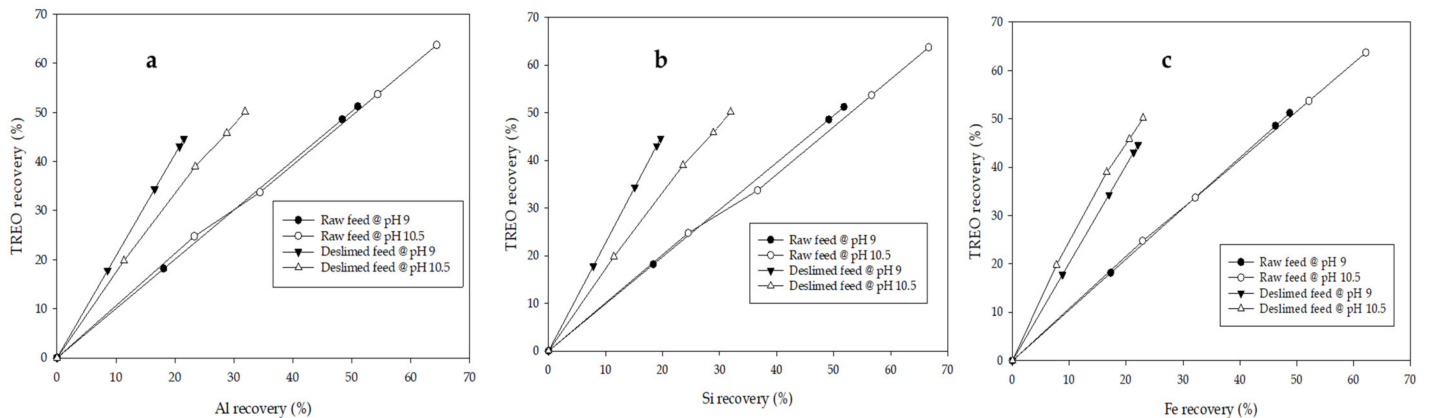


Figure 11. TREO (a) Al, (b) Si, and (c) Fe species selectivity analyses. R^2 values obtained in all the analyses were ~1, demonstrating good reliance of the data obtained from the plots.

Table 8. Summary of REE–gangue species selectivity analyses.

Relation	Selectivity Index		R^2	
	Raw	Deslimed	Raw	Deslimed
Al-TREO @ pH 9	1.00	2.07	1.00	1.00
Al-TREO @ pH 10.5	0.98	1.57	0.99	0.99
Si-TREO @ pH 9	0.99	2.27	1.00	1.00
Si-TREO @ pH 10.5	0.95	1.57	0.99	0.99
Fe-TREO @ pH 9	1.05	2.02	1.00	1.00
Fe-TREO @ pH 10.5	1.02	2.18	0.99	0.99

4.5. Effect of Depressants

In order to assess the impact of depressants in REE recovery from the ore, data obtained in the cleaning stage of Flowsheet III were compared. Generally, the depressants were effective in inhibiting gangue minerals recovery in the cleaning stage as expected. This was consistent with results obtained in previous studies reported in the literature. Notably, the results suggested a significant proportion of TREO was lost to the tailings in Flowsheet III at pH 10.5, indicating that the depressants used in the present study have deleterious effects on REE minerals recovery in strong alkaline pulp (pH > 9.5) conditions. In effect, the depressants’ action was affected by pulp pH, with a better selectivity for REE minerals occurring at pH 9, hence the better TREO concentrate grade obtained in the cleaning stage of Flowsheet III at pH 9.

4.6. TREO Grade–Recovery Relationship and Implications

Figure 12 compares the performance of single- and multi-stage flotation of REE minerals from the ore. Flotation tests conducted on the raw feed presented the poorest performance in terms of TREO upgrade, although the recoveries were high. On the other hand, desliming followed by the flotation of the material presented significant improvement in TREO upgrade, although this resulted in some REE value loss. Figure 12 shows a non-linear relationship between the two parameters. The haphazard grade–recovery relationship suggested that there is an opportunity to further maximize both TREO recovery and grade

through further studies. For instance, the relative impacts of elevated temperatures, agitation rates, different collectors (hydroxamate, phosphoric acid, sodium dodecylsulphate) and depressants, high intensity conditioning (HIC), air flow rates, and pulp density may be investigated as part of optimization studies in future work [21,23,51,57–60]. With REE mostly mineralized with bastnäsite, a paramagnetic mineral, and diamagnetic clay and silicate gangue minerals occupying the bulk of the material, there is an opportunity to investigate the use of magnetic separation processes [1,18,61,62].

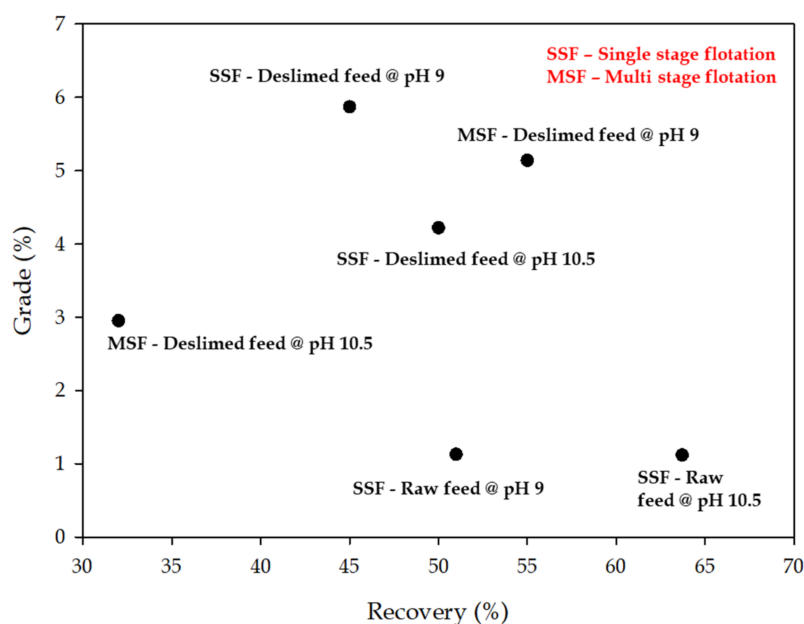


Figure 12. TREO grade–recovery curve comparing the performance of different flotation methods tested in this study.

Overall, the results of this study are encouraging and potentially significant in view of the massive amount of complex low-grade saprolite ores containing REE in Australia and other parts of the world, for which there is currently a paucity of data on the technical feasibility of recovering valuable REE minerals. The final concentrates from Flowsheets II and III could serve as both pyro- and hydrometallurgical feed for REE extraction. However, further processing of the material to maximize TREO concentrate grade while reducing penalty elements (e.g., Fe) will present significant economic gains.

5. Conclusions

A complex, low-grade saprolite ore was characterized to determine the mode of occurrence and distribution of REE and gangue minerals and subsequently processed using different flotation methods. The ore contains 1.142% TREO, along with 22.25% Si, 13.8% Al, and 2.83% Fe. QEMSCAN data demonstrated that bastnäsite is the major REE bearing mineral in the ore, with the other REE phases adsorbed onto clay minerals. These REE phases were not identified by XRD, probably due to the closely matching XRD spectra with major gangue minerals and their low concentrations relative to the gangue minerals.

In the flotation study, three different flowsheets were tested at pulp pH 9 and 10.5, respectively. Overall, REE minerals recovery was affected by changes in pulp pH, the introduction of depressants, and desliming stage. Flotation flowsheet including desliming followed by single stage flotation at pH 9, produced the best results in terms of upgrade where 5.87% TREO concentrate grade was obtained at 45% recovery. The highest TREO recovery of 68% at a concentrate grade of 1.19% was obtained when the raw feed was processed at pH 10.5. Flowsheet III at pH 9 produced the highest flotation efficiency by recovering 55% TREO at a concentrate grade of 5.14% from deslimed feed.

Characterization of the deslimed flotation feed and concentrate (from Flowsheet III at pH 9) showed that REE minerals were effectively enriched, with clay and silicate gangue minerals forming the bulk of the materials. The high clay and silicate gangue recoveries observed were mainly attributed to their free, fine-, or ultrafine nature. This study also showed that the depressants' performance was affected by pulp pH, where the depressants had a deleterious impact on REE minerals recovery and selectivity at pH 10.5.

The promising results obtained by using these relatively simple flotation methods suggest that the tested processes could be easily integrated into proposed and existing operations to recover REE minerals as by-products of gold and copper extraction from the ore. The non-linear, scattered relation between TREO grade and recovery, suggests there is an opportunity to improve the results obtained in this work through testing other flotation parameters and using magnetic separation processes.

Author Contributions: Conceptualization, methodology, writing—original draft, review and editing, formal analysis, investigation, data curation: G.B.A.-W. and J.A.-M.; conceptualization, writing—review and editing, project administration and supervision: B.J. and W.S. All authors have read and agreed to the published version of the manuscript.

Funding: This research was funded by Havalah Resources Limited, South Australia.

Acknowledgments: George Blankson Abaka-Wood and William Skinner wish to acknowledge support from the Australian Research Council for the ARC Centre of Excellence for Enabling Eco-Efficient Beneficiation of Minerals, grant number CE200100009.

Conflicts of Interest: The authors declare no conflict of interest.

References

1. Abaka-Wood, G.B.; Addai-Mensah, J.; Skinner, W. The Use of Mining Tailings as Analog of Rare Earth Elements Resources: Part 1—Characterization and Preliminary Separation. *Miner. Process. Extr. Met. Rev.* **2021**, *43*, 701–715. [[CrossRef](#)]
2. Geoscience-Australia. *Australia's Identified Mineral Resources 2013*; Geoscience Australia: Canberra, Australia, 2014; pp. 107–115.
3. Dang, D.H.; Thompson, K.A.; Ma, L.; Nguyen, H.Q.; Luu, S.T.; Duong, M.T.N.; Kernaghan, A. Toward the circular economy of Rare Earth Elements: A review of abundance, extraction, applications, and environmental impacts. *Arch. Environ. Contam. Toxicol.* **2021**, *81*, 521–530. [[CrossRef](#)]
4. U.S. Geological Survey. *Geological Survey. Mineral Commodity Summaries 2022*; U.S. Geological Survey: Reston, VA, USA, 2022; p. 206.
5. Abaka-Wood, G.B.; Ehrig, K.; Addai-Mensah, J.; Skinner, W. Recovery of Rare Earth Elements Minerals from Iron-Oxide-Silicate-Rich Tailings: Research Review. *Eng* **2022**, *3*, 259–275. [[CrossRef](#)]
6. Zhou, B.; Li, Z.; Chen, C. Global potential of rare earth resources and rare earth demand from clean technologies. *Minerals* **2017**, *7*, 203. [[CrossRef](#)]
7. Barteková, E.; Kemp, R. National strategies for securing a stable supply of rare earths in different world regions. *Resour. Policy* **2016**, *49*, 153–164. [[CrossRef](#)]
8. Ilankoon, I.; Dushyantha, N.; Mancheri, N.; Edirisinghe, P.; Neethling, S.; Ratnayake, N.; Rohitha, L.; Dissanayake, D.; Premasiri, H.; Abeyasinghe, A.; et al. Constraints to rare earth elements supply diversification: Evidence from an industry survey. *J. Clean. Prod.* **2022**, *331*, 129932. [[CrossRef](#)]
9. Kim, H.-M.; Jariwala, D. *The Not-So-Rare Earth Elements: A Question of Supply and Demand*; University of Pennsylvania: Philadelphia, PA, USA, 2021; p. 20.
10. Charalampides, G.; Vatalis, K.I.; Apostoplos, B.; Ploutarch-Nikolas, B. Rare earth elements: Industrial applications and economic dependency of Europe. *Procedia Econ. Financ.* **2015**, *24*, 126–135. [[CrossRef](#)]
11. Nassar, N.T.; Du, X.; Graedel, T.E. Criticality of the rare earth elements. *J. Ind. Ecol.* **2015**, *19*, 1044–1054. [[CrossRef](#)]
12. Imholte, D.; Nguyen, R.; Vedantam, A.; Brown, M.; Iyer, A.; Smith, B.; Collins, J.; Anderson, C.; O'Kelley, B. An assessment of US rare earth availability for supporting US wind energy growth targets. *Energy Policy* **2018**, *113*, 294–305. [[CrossRef](#)]
13. Wang, Z.-Y.; Fan, H.-R.; Zhou, L.; Yang, K.-F.; She, H.-D. Carbonatite-related REE deposits: An overview. *Minerals* **2020**, *10*, 965. [[CrossRef](#)]
14. Guo, D.; Liu, Y. Occurrence and geochemistry of bastnäsite in carbonatite-related REE deposits, Mianning–Dechang REE belt, Sichuan Province, SW China. *Ore Geol. Rev.* **2019**, *107*, 266–282. [[CrossRef](#)]
15. Estrade, G.; Marquis, E.; Smith, M.; Goodenough, K.; Nason, P. REE concentration processes in ion adsorption deposits: Evidence from the Ambohimirahavavy alkaline complex in Madagascar. *Ore Geol. Rev.* **2019**, *112*, 103027. [[CrossRef](#)]
16. Jordens, A.; Cheng, Y.P.; Waters, K.E. A review of the beneficiation of rare earth element bearing minerals. *Miner. Eng.* **2013**, *41*, 97–114. [[CrossRef](#)]

17. Xu, C.; Zhong, C.; Lyu, R.; Ruan, Y.; Zhang, Z.; Chi, R. Process mineralogy of Weishan rare earth ore by MLA. *J. Rare Earths* **2019**, *37*, 334–338. [[CrossRef](#)]
18. Abaka-Wood, G.B.; Zanin, M.; Addai-Mensah, J.; Skinner, W. Recovery of rare earth elements minerals from iron oxide–silicate rich tailings—Part 1: Magnetic separation. *Miner. Eng.* **2019**, *136*, 50–61. [[CrossRef](#)]
19. Abaka-Wood, G.; Addai-Mensah, J.; Skinner, W. The concentration of rare earth elements from coal fly ash. *J. South. Afr. Inst. Min. Metall.* **2022**, *122*, 21–28. [[CrossRef](#)]
20. Filippov, L.O.; Dehaine, Q.; Filippova, I.V. Rare earths (La, Ce, Nd) and rare metals (Sn, Nb, W) as by-products of kaolin production—Part 3: Processing of fines using gravity and flotation. *Miner. Eng.* **2016**, *95*, 96–106. [[CrossRef](#)]
21. Satur, J.V.; Calabria, B.P.; Hoshino, M.; Morita, S.; Seo, Y.; Kon, Y.; Takagi, T.; Watanabe, Y.; Mutele, L.; Foya, S. Flotation of rare earth minerals from silicate–hematite ore using tall oil fatty acid collector. *Miner. Eng.* **2016**, *89*, 52–62. [[CrossRef](#)]
22. Pavez, O.; Brandao, P.; Peres, A. Adsorption of oleate and octyl-hydroxamate on to rare-earths minerals. *Miner. Eng.* **1996**, *9*, 357–366. [[CrossRef](#)]
23. Chelgani, S.C.; Rudolph, M.; Leistner, T.; Gutzmer, J.; Peuker, U. A review of rare earth minerals flotation: Monazite and xenotime. *Int. J. Min. Sci. Technol.* **2015**, *25*, 877–883. [[CrossRef](#)]
24. Abaka-Wood, G.B.; Fosu, S.; Addai-Mensah, J.; Skinner, W. Flotation recovery of rare earth oxides from hematite–quartz mixture using sodium oleate as a collector. *Miner. Eng.* **2019**, *141*, 105847. [[CrossRef](#)]
25. Aylmore, M.G.; Muir, D.M. Thiosulfate leaching of gold—A review. *Miner. Eng.* **2001**, *14*, 135–174. [[CrossRef](#)]
26. Asamoah, R.K.; Skinner, W.; Addai-Mensah, J. Alkaline cyanide leaching of refractory gold flotation concentrates and bio-oxidised products: The effect of process variables. *Hydrometallurgy* **2018**, *179*, 79–93. [[CrossRef](#)]
27. Du Plessis, C.; Lambert, H.; Gärtner, R.S.; Ingram, K.; Slabbert, W.; Eksteen, J.J. Lime use in gold processing—A review. *Miner. Eng.* **2021**, *174*, 107231. [[CrossRef](#)]
28. Abaka-Wood, G.B.; Addai-Mensah, J.; Skinner, W. A study of selective flotation recovery of rare earth oxides from hematite and quartz using hydroxamic acid as a collector. *Adv. Powder Technol.* **2018**, *29*, 1886–1899. [[CrossRef](#)]
29. Fuerstenau, M.C.; Somasundaran, P. *Flotation in Principles of Mineral Processing*; Fuerstenau, M.C., Han, K.N., Eds.; SME: New York, NY, USA, 2003; pp. 245–300.
30. Hoang, D.H.; Heitkam, S.; Kupka, N.; Hassanzadeh, A.; Peuker, U.A.; Rudolph, M. Froth properties and entrainment in lab-scale flotation: A case of carbonaceous sedimentary phosphate ore. *Chem. Eng. Res. Des.* **2019**, *142*, 100–110. [[CrossRef](#)]
31. Duarte, A.; Grano, S. Mechanism for the recovery of silicate gangue minerals in the flotation of ultrafine sphalerite. *Miner. Eng.* **2007**, *20*, 766–775. [[CrossRef](#)]
32. Taner, H.A.; Onen, V. Control of clay minerals effect in flotation. A review. *E3S Web Conf.* **2016**, *8*, 01062. [[CrossRef](#)]
33. Andrews, W.; Collins, D.; Hollick, C. The flotation of rare earths—A Contribution to industrial hygiene. In Proceedings of the 1990 AusIMM New Zealand Branch Annual Conference: The Mineral Industry in New Zealand, Rotorua, New Zealand, 18–21 March 1990.
34. Pereira, C.A.; Peres, A.E.C. Flotation concentration of a xenotime pre-concentrate. *Miner. Eng.* **1997**, *10*, 1291–1295. [[CrossRef](#)]
35. Moldoveanu, G.A.; Papangelakis, V.G. An overview of rare-earth recovery by ion-exchange leaching from ion-adsorption clays of various origins. *Miner. Mag.* **2016**, *80*, 63–76. [[CrossRef](#)]
36. Ram, R.; Becker, M.; Brugger, J.; Etschmann, B.; Burcher-Jones, C.; Howard, D.; Kooyman, P.J.; Petersen, J. Characterisation of a rare earth element-and zirconium-bearing ion-adsorption clay deposit in Madagascar. *Chem. Geol.* **2019**, *522*, 93–107. [[CrossRef](#)]
37. Feng, X.; Onel, O.; Council-Troche, M.; Noble, A.; Yoon, R.-H.; Morris, J.R. A study of rare earth ion-adsorption clays: The speciation of rare earth elements on kaolinite at basic pH. *Appl. Clay Sci.* **2021**, *201*, 105920. [[CrossRef](#)]
38. Gong, J.; Peng, Y.; Bouajila, A.; Ourriban, M.; Yeung, A.; Liu, Q. Reducing quartz gangue entrainment in sulphide ore flotation by high molecular weight polyethylene oxide. *Int. J. Miner. Process.* **2010**, *97*, 44–51. [[CrossRef](#)]
39. Corin, K.; McFadzean, B.; Shackleton, N.; O’Connor, C. Challenges related to the processing of fines in the recovery of platinum group minerals (PGMs). *Minerals* **2021**, *11*, 533. [[CrossRef](#)]
40. Derhy, M.; Taha, Y.; Hakkou, R.; Benzaazoua, M. Review of the main factors affecting the flotation of phosphate ores. *Minerals* **2020**, *10*, 1109. [[CrossRef](#)]
41. Cheng, T.-W.; Holtham, P.; Tran, T. Froth flotation of monazite and xenotime. *Miner. Eng.* **1993**, *6*, 341–351. [[CrossRef](#)]
42. Zhang, W.; Honaker, R.; Groppo, J. Concentration of rare earth minerals from coal by froth flotation. *Miner. Met. Process.* **2017**, *34*, 132–137. [[CrossRef](#)]
43. Joseph-Soly, S.; Quast, K.; Connor, J.N. Effects of Eh and pH on the oleate flotation of iron oxides. *Miner. Eng.* **2015**, *83*, 97–104. [[CrossRef](#)]
44. Fan, G.; Wang, L.; Cao, Y.; Li, C. Collecting agent–mineral interactions in the reverse flotation of iron ore: A brief review. *Minerals* **2020**, *10*, 681. [[CrossRef](#)]
45. Jung, R.F.; James, R.O.; Healy, T.W. Adsorption, precipitation, and electrokinetic processes in the iron oxide (Goethite)—Oleic acid—Oleate system. *J. Colloid Interface Sci.* **1987**, *118*, 463–472. [[CrossRef](#)]
46. Zhou, C.H.; Keeling, J. Fundamental and applied research on clay minerals: From climate and environment to nanotechnology. *Appl. Clay Sci.* **2013**, *74*, 3–9. [[CrossRef](#)]
47. Fuerstenau, M.; Cummins, W. The role of basic aqueous complexes in anionic flotation of quartz. *Trans. AIME* **1967**, *238*, 196.
48. Trahar, W. A rational interpretation of the role of particle size in flotation. *Int. J. Miner. Process.* **1981**, *8*, 289–327. [[CrossRef](#)]

49. Wang, L.; Peng, Y.; Runge, K.; Bradshaw, D. A review of entrainment: Mechanisms, contributing factors and modelling in flotation. *Miner. Eng.* **2015**, *70*, 77–91. [[CrossRef](#)]
50. Wang, L.; Runge, K.; Peng, Y.; Vos, C. An empirical model for the degree of entrainment in froth flotation based on particle size and density. *Miner. Eng.* **2016**, *98*, 187–193. [[CrossRef](#)]
51. Abaka-Wood, G.B.; Zanin, M.; Addai-Mensah, J.; Skinner, W. The upgrading of rare earth oxides from iron-oxide silicate rich tailings: Flotation performance using sodium oleate and hydroxamic acid as collectors. *Adv. Powder Technol.* **2018**, *29*, 3163–3172. [[CrossRef](#)]
52. Whitworth, A.J.; Forbes, E.; Verster, I.; Jokovic, V.; Awatey, B.; Parbhakar-Fox, A. Review on advances in mineral processing technologies suitable for critical metal recovery from mining and processing wastes. *Clean. Eng. Technol.* **2022**, *7*, 100451. [[CrossRef](#)]
53. Chen, J.; Chimonyo, W.; Peng, Y. Flotation behaviour in reflux flotation cell—A critical review. *Miner. Eng.* **2022**, *181*, 107519. [[CrossRef](#)]
54. Jiang, K.; Dickinson, J.; Galvin, K. The kinetics of fast flotation using the reflux flotation cell. *Chem. Eng. Sci.* **2019**, *196*, 463–477. [[CrossRef](#)]
55. Eskanlou, A.; Huang, Q.; Zhang, P. De-sliming followed by froth flotation for the recovery of phosphorus and enrichment of rare earth elements from Florida waste clay. *Resour. Conserv. Recycl.* **2022**, *178*, 106049. [[CrossRef](#)]
56. Rabatho, J.P.; Tongamp, W.; Shibayama, A.; Takasaki, Y.; Nitta, S.; Imai, T. Investigation of a flotation process with de-sliming and attrition to upgrade and recover Cu and Mo from a Cu-Mo flotation tailing. *Mater. Trans.* **2011**, *52*, 746–752. [[CrossRef](#)]
57. Hart, B.R.; Dimov, S.; Xia, L. REE bearing mineral recovery: A microflotation and surface chemistry study using hydroxamate collectors and citric acid. In Proceedings of the XXVII International Mineral Processing Congress, San Tiago, Chile, 20–24 October 2014.
58. Filippov, L.; Severov, V.; Filippova, I. An overview of the beneficiation of iron ores via reverse cationic flotation. *Int. J. Miner. Process.* **2014**, *127*, 62–69. [[CrossRef](#)]
59. Li, R.; Marion, C.; Espiritu, E.; Multani, R.; Sun, X.; Waters, K. Investigating the use of an ionic liquid for rare earth mineral flotation. *J. Rare Earths* **2021**, *39*, 866–874. [[CrossRef](#)]
60. Espiritu, E.R.L.; Naseri, S.; Waters, K.E. Surface chemistry and flotation behavior of dolomite, monazite and bastnäsite in the presence of benzohydroxamate, sodium oleate and phosphoric acid ester collectors. *Colloids Surf. A Physicochem. Eng. Asp.* **2018**, *546*, 254–265. [[CrossRef](#)]
61. Jordens, A.; Sheridan, R.S.; Rowson, N.A.; Waters, K.E. Processing a rare earth mineral deposit using gravity and magnetic separation. *Miner. Eng.* **2014**, *62*, 9–18. [[CrossRef](#)]
62. Park, I.; Kanazawa, Y.; Sato, N.; Galtchandmani, P.; Jha, M.K.; Tabelin, C.B.; Jeon, S.; Ito, M.; Hiroyoshi, N. Beneficiation of low-grade rare earth ore from Khalzan Buregtei deposit (Mongolia) by magnetic separation. *Minerals* **2021**, *11*, 1432. [[CrossRef](#)]